

Escape from a zero current state in a one dimensional array of Josephson junctions

K. Andersson* and D. B. Haviland

*Nanostructure physics, KTH
AlbaNova universitetscentrum*

S-106 91 Stockholm, SWEDEN

(Dated: November 2, 2018)

A long one dimensional array of small Josephson junctions exhibits Coulomb blockade of Cooper pair tunneling. This zero current state exists up to a switching voltage, V_{sw} , where there is a sudden onset of current. In this paper we present histograms showing how V_{sw} changes with temperature for a long array and calculations of the corresponding escape rates. Our analysis of the problem is based on the existence of a voltage dependent energy barrier and we do not make any assumptions about its shape. The data divides up into two temperature regimes, the higher of which can be explained with Kramers thermal escape model. At low temperatures the escape becomes independent of temperature.

PACS numbers: 73.23.Hk, 74.50.+r, 73.23.-b, 05.40.Jc

Escape from a metastable state can be used to describe a wide variety of physical phenomenon, from solid state diffusion [1] to magnetic switching [2], and has for a long time attracted attention from both a theoretical and an experimental point of view (for a review see e.g. [3]). Thermal escape over an energy barrier was studied theoretically by Kramers in the 1940s [4]. More recently, the influence of quantum tunneling on the escape process has been an important means of studying the quantum behavior of macroscopic variables. In this context, escape from the zero voltage state of a Josephson junction has been thoroughly studied [5, 6]. In this paper we adopt the Kramers model to analyze the escape from the zero *current* state of a one dimensional array of Josephson junctions exhibiting a Coulomb blockade of Cooper pair tunneling. We find that the escape process is well described by thermal activation at higher temperatures, but at lower temperatures the escape process becomes independent of temperature.

In the Kramers thermal activation model, the rate of escape Γ , over an energy barrier ΔU , is given by,

$$\Gamma = \kappa \frac{\omega_p}{2\pi} \exp\left(-\frac{\Delta U}{k_B T}\right) \quad (1)$$

where k_B is Boltzmann's constant and ω_p is the attempt frequency, or the frequency of small oscillations around the metastable minimum. The dimensionless transmission factor κ depends on the shape of the barrier and the damping [3]. This model has been applied to single Josephson junctions, where the energy barrier is a one dimensional tilted washboard potential, and the tilt is controlled by bias current applied to the junction, $\Delta U(I)$ [5, 6, 7]. Long Josephson junctions (modeled by parallel arrays of single junctions) have also been studied, and in this case the escape is from a metastable minimum in a multi-dimensional space [8]. All Josephson junction systems studied with this technique thus far exhibit a zero voltage state with a finite supercurrent, above which the system switches to a finite voltage state. A voltage across

the junction develops when the superconducting phase, ϕ , across the junction escapes over the Josephson potential energy barrier to a free-running state ($V \propto \dot{\phi}$). The escape can be due to thermal activation or quantum tunneling of the junction phase through the energy barrier. The important quantities for the escape problem are the height of the Josephson potential and the attempt frequency, which are given in terms of other junction parameters such as normal state resistance, superconducting energy gap and junction capacitance. This escape description applied to the Josephson junction is based on the classical dynamics of the Josephson phase, as embodied in the Josephson effect.

In this letter we analyze the Coulomb blockade of Cooper pair tunneling, a phenomena which is in many ways dual to the Josephson effect [9, 10]. In one-dimensional arrays of small capacitance Josephson junctions, the coupling of the Josephson phase to dissipation can be manipulated so that there are very large quantum fluctuations of the phase [11]. In this case, the number of Cooper pairs becomes a classical variable, and transport through the array is described by a Coulomb blockade, where a zero current state persists until a switching voltage is exceeded. One- and two-dimensional arrays of small capacitance Josephson junctions have been well studied in the context of the superconductor-insulator transition [12]. Here we focus on analysis of transport properties of a 1D array deep in the insulating regime. We do this by studying fluctuations of the switching voltage and analyzing them in the context of the Kramers model. This is the first time to our knowledge that such an experimental study has been carried out on Cooper pair tunneling in the insulating regime.

The array is made of Al, with Al_2O_3 tunnel barriers, on a SiO_2 surface using the standard two angle evaporation technique [13]. Electron beam lithography was used to define the mask pattern, which made 400 junctions in series. Each junction had dimensions $100\text{nm} \times 150\text{nm}$,

and each island was connected by two junctions in parallel, forming a Superconducting QUantum Interference Device (SQUID). The charging energy E_C of the SQUID was $E_C \equiv e^2/2C = 59\mu\text{eV}$, where we have assumed a specific capacitance of $45\text{fF}/\mu\text{m}^2$ [14]. The junctions normal state resistance R_n controls the Josephson energy at zero magnetic field, $E_{J0} = (R_Q/R_n)\Delta/2$ where $\Delta = 200\mu\text{eV}$ is the superconducting energy gap of Al. For the array presented here we had $R_n = 4.6\text{k}\Omega$ per SQUID, or $E_{J0} = 142\mu\text{eV}$.

The advantage of the SQUID geometry is that we can tune the Josephson coupling by applying a magnetic flux to the SQUID loops $E_J = E_{J0} |\cos(\pi BA/\Phi_0)|$, where B is the magnetic field perpendicular to the SQUID loop, A is the effective area of the loop (in this case $0.85 \times 0.2\mu\text{m}^2$) and $\Phi_0 = h/2e = 2.06 \times 10^{-15}\text{Wb}$ is the superconducting flux quantum.

The arrays were measured in a dilution refrigerator with well filtered measurement lines. The chip is mounted on a socket which is in turn mounted in a RF tight copper can. The leads into the can are 1 meter of Thermocoax which attenuates at high frequency [15]. The can and filtered leads are mounted at the lowest temperature. The bonding pads and contact leads on the chip were fabricated of Au to within $50\mu\text{m}$ of the array edge. Low noise and high input impedance amplifiers were used to measure the voltage and current.

In Fig. 1 we see a typical current-voltage (I - V) characteristic of a 1D array in the Coulomb blockade state. When increasing the bias voltage across the array the Coulomb blockade state is interrupted by a sudden onset of current at the switching voltage, V_{sw} . Subsequently lowering the bias voltage across the array, the Cooper pairs are retrapped at a voltage $V_r < V_{sw}$, giving rise to a hysteresis in the current-voltage characteristics. The retrapping voltage remains the same at fixed magnetic field, whereas the switching voltage fluctuates. Both V_{sw} and V_r depend on E_J and are modulated with magnetic field having a period associated with one flux quantum in each SQUID loop, as can be seen in the inset of Fig. 1. This modulation is clear evidence that the switching voltage is associated with the Cooper pair tunneling in the array.

By making 10^4 sweeps of the bias voltage and each time registering the switching voltage V_{sw} , we obtain a switching histogram representing the probability distribution $P(V)$ from which the escape rate can be calculated through the formula [7],

$$\Gamma(V) = \frac{1}{\Delta V} \frac{dV}{dt} \ln \left(\frac{\sum_{v \geq V} P(v)}{\sum_{v \geq V + \Delta V} P(v)} \right) \quad (2)$$

where dV/dt is the ramp rate of the voltage and ΔV is the width of the bins in the histogram.

To establish that the switching process is indeed sensitive to the applied voltage, we have varied the sweep

rate by changing the frequency of our triangular sweep between 5 and 200Hz, while keeping the amplitude of the sweep constant at 1.2mV. For lower sweep rates the histogram shifted to lower voltages as we are less likely to reach higher voltages before escape occurs. However, when the escape rate $\Gamma(V)$ was calculated according to (2) and comparison was made for different sweep rates, we found see that for sweep rates lower than 0.12V/s, the escape rate at a given voltage was essentially unaffected by the sweep rate. We also found that for sweep rates higher than 0.12V/s, the escape rate $\Gamma(V)$ becomes sensitive to the sweep rate. This limitation on sweep rate was set by the biasing and current measurement circuit together with the stray capacitance of the cryostat leads. From this analysis we conclude that the switching process, when measured with sweep speed below 0.12V/s, is truly a voltage dependent escape problem. We also investigated if the switching process is affected by the time spent in the dissipative (finite current) state by putting in a delay and waiting at zero voltage between successive ramps. The result of this investigation was that the switching histogram for fixed sweep rate and temperature remained the same, independent of delay time.

Figure 2 shows a selected number of histograms at different temperatures. The inset of Fig. 2 shows how the voltage value at the peak of the histogram changes versus temperature. At temperatures above about 130mK, the displacement of the peak position is proportional to the temperature. We also see that the width of the distribution increases as the temperature is decreased. The retrapping voltage put a lower limit on the switching voltage and thereby sets a maximum temperature of about 180mK. Therefore we limit ourselves to temperatures between 170mK and the base temperature of the cryostat,

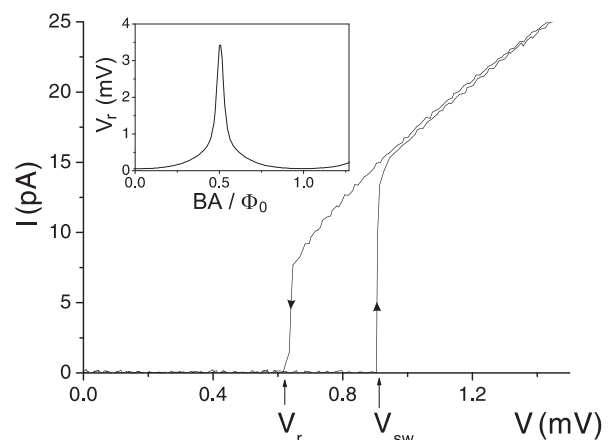


FIG. 1: Current voltage characteristics of a typical long one dimensional array of Josephson junctions. Voltage bias gives a hysteretic $I - V$ curve, with a switching voltage, V_{sw} , and the retrapping voltage, V_r . The arrows on the curve indicate the direction of the sweep. The inset shows how V_r is modulated with B .

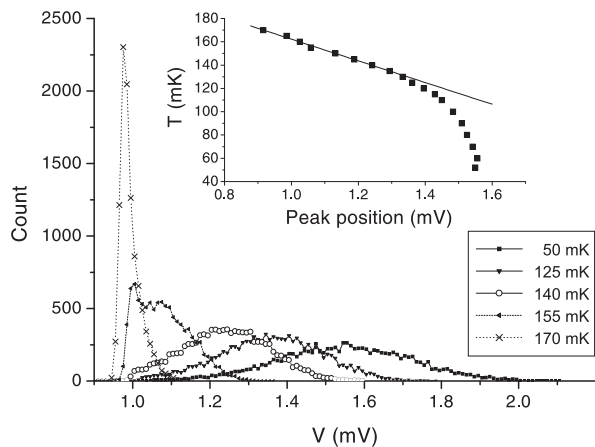


FIG. 2: A selection of histograms containing 10^4 switching events, each at different temperatures. As the temperature increases the histogram shifts towards lower voltages. At high temperatures it is evident how the retrapping current affects the histogram as V_{sw} gets closer to V_r . The inset shows how the peak of the histogram moves with temperature.

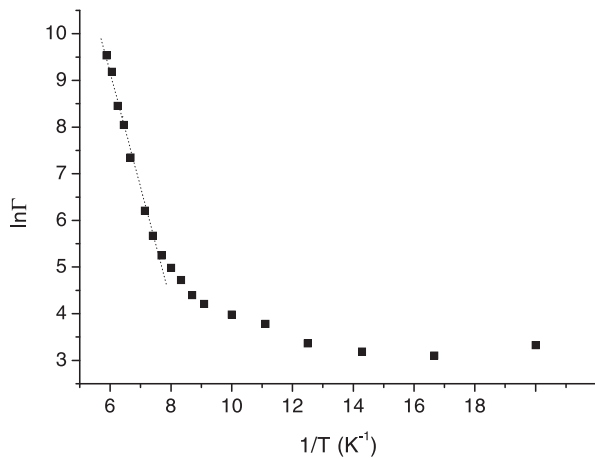


FIG. 3: $\ln \Gamma$ versus the inverse temperature at 1.1 mV. Two temperature regimes are seen, the higher of which follows the thermal escape model.

about 50 mK.

From the histograms we can determine the escape rate $\Gamma(V)$ via equation (2). In Fig. 3 we have plotted $\Gamma(V = 1.1 \text{ mV})$ versus $1/T$. Here we see that in the high temperature region between 170 mK and 130 mK, the data is well described by Kramers' model of thermally activated escape, equation (1). However at low temperatures, below ca 130 mK, the escape rate crosses over to a different behavior, becoming independent of temperature at the lowest temperature attainable. By extrapolating the linear fit in the low temperature region shown in Fig. 3, we find the intersection with the $\ln \Gamma$ -axis and make an estimate of the factor, $\kappa\omega_p$ of the order of $10^9 - 10^{10}$ Hz. An alternative way to find $\kappa\omega_p$, which uses the data at all voltages, is to extract the energy barrier $\Delta U(V)$ from

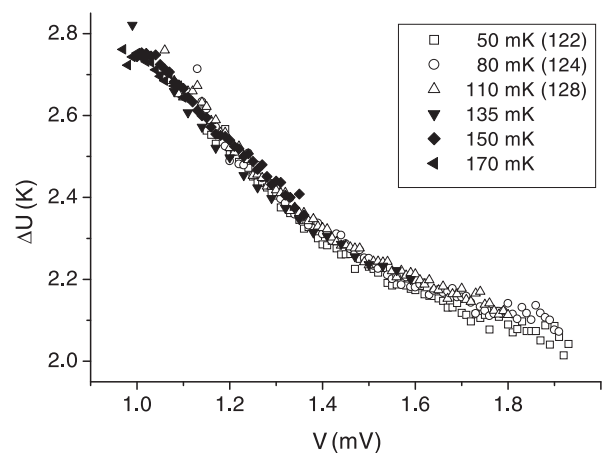


FIG. 4: Selected curves showing how all data can be reduced to a single $\Delta U(V)$ curve in eq. (1), with $\kappa\omega_p = 80 \text{ GHz}$. The low temperature curves with the open symbols are fitted with an effective temperatures indicated in the parenthesis.

the escape rate $\Gamma(V)$ via equation (1). We then adjust $\kappa\omega_p$ so that the data at all temperatures fall on to a single $\Delta U(V)$ curve. We find that in the high temperature region between 170 mK and 130 mK, the data collapse on to one curve for $\kappa\omega_p = 80 \text{ GHz}$ as is shown in Fig. 4.

We note that this method of determining $\kappa\omega_p$ differs from the traditional analysis of escape from the superconducting state of Josephson junctions. In the superconducting case we have a well established model for the energy barrier, and to an excellent approximation, escape from the cubic potential can be assumed. The cubic potential results in a straight line plot of $(\ln(\omega_p/2\pi\Gamma))^{2/3}$ versus the bias current [5]. If we follow this analysis and plot $(\ln(\omega_p/2\pi\Gamma))^{2/3}$ versus bias voltage in the temperature range 130 – 170 mK using the value $\kappa\omega_p = 80 \text{ GHz}$, we also find a straight line. However, the limited width of the distribution and the small temperature range make it difficult to say if the data follows the theoretical predictions (slope $\propto T^{-2/3}$ and intersect with the x-axis at V_0). We can, however, conclude that the qualitative behavior is correct.

Thus the data are well described by the thermal activation model in the high temperature regime with $\kappa\omega_p = 80 \text{ GHz}$. Fixing the value of $\kappa\omega_p = 80 \text{ GHz}$, we can then analyze the low temperature regime ($T < 130 \text{ mK}$) by adjusting the temperature in equation (1) to find an effective temperature. Following this procedure, all data for all voltage and temperature can be reduced to one $\Delta U(V)$ as shown for a few selected temperatures in Fig. 4. The effective temperature, T_{eff} , is plotted versus the thermometer temperature in Fig. 5. Here we can see how the data can be described by the thermal escape model if an effective temperature is assumed that reaches a minimum value of 122 mK as the cryostat is cooled towards base temperature.

There can be several reasons for deviation from the thermal activation model at low temperatures. The escape temperature of 122mK may be a result some source of heating of the sample, so that the sample is not in equilibrium with our thermometer. We can rule out self-heating by the current in the sample [16] because we are measuring escape from a zero current state, where there is no dissipation in the sample. The low temperature escape may also be influenced by RF and microwave noise reaching the sample through the filtered measurement leads. Another possibility is that the escape process at low temperatures is determined by macroscopic quantum tunneling (MQT).

MQT rates have been calculated for the cubic potential at $T = 0$ [17],

$$T_{esc} \approx \frac{\hbar\omega_p/k_B}{7.2(1 + 0.87/Q)} \quad (3)$$

where Q is the damping factor. Assuming moderate to weak damping ($Q \gg 1$) and $\kappa \sim 1$ we can calculate an MQT escape temperature $T_{esc} \sim 85\text{mK}$, which is in reasonable agreement with the effective escape temperature found with our method of analysis. However, similar measurements and analysis on a slightly shorter array found a much lower $\kappa\omega_p \approx 10\text{MHz}$. This would result in $T_{esc} \sim 10\mu\text{K}$ in the MQT model, in poor agreement with the effective escape temperature $T_{eff}(0) \approx 100\text{mK}$ found in the data analysis.

In conclusion, we have studied the onset of finite current in long, one-dimensional Josephson junction arrays in the Coulomb blockade state. By analyzing the temperature dependence of fluctuations of the switching voltage for the onset of finite current, we have shown that this onset can be described by the Kramers model for thermally activated escape over an energy barrier, where the

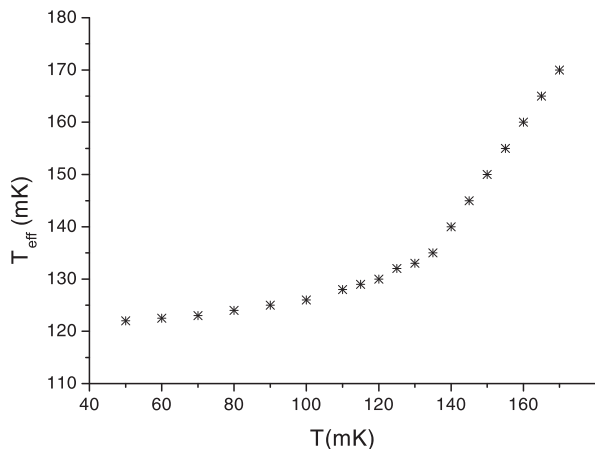


FIG. 5: The effective temperature, T_{eff} , is plotted versus the thermometer temperature, T . At high temperatures $T_{eff} \equiv T$. At low temperatures T_{eff} was inferred by mapping all data to the same $\Delta U(V)$ curve.

barrier height depends on the bias voltage. The data fall into two temperature regimes. At high temperature thermal activation applies, but at low temperature an effective temperature must be assumed to fit the data to the Kramers model. The low temperature behavior could be the result of external noise causing the escape over the barrier, or possibly, macroscopic quantum tunneling through the barrier.

We would like to acknowledge helpful discussions with R. Kautz and T. Duty, and financial support from the NFR, Göran Gustafsson Foundation and the EU project SQUBIT.

* Electronic address: karina@nanophys.kth.se

- [1] R. DiFoggio and R. Gomer, Phys. Rev. B **25**, 3490 (1982).
- [2] J. Z. Sun, J. C. Slonczewski, P. L. Trouilloud, D. Abraham, I. Bacchus, W. J. Gallagher, J. Hummel, Y. Lu, G. Wright, S. S. P. Parkin, et al., Appl. Phys. Lett. **78**, 4004 (2001).
- [3] P. Hänggi, P. Talkner, and M. Borkovec, Rev. Mod. Phys. **62**, 251 (1990).
- [4] H. A. Kramers, Physica (Utrecht) **7**, 284 (1940).
- [5] J. M. Martinis, M. H. Devoret, and J. Clarke, Phys. Rev. B **35**, 4682 (1987).
- [6] M. H. Devoret, D. Esteve, C. Urbina, J. Martinis, A. Cleland, and J. Clark, *Quantum Tunnelling in Condensed Matter* (Elsevier Science Publishers, 1992), chap. 6, pp. 313–345.
- [7] T. A. Fulton and L. N. Dunkleberger, Phys. Rev. B **9**, 4760 (1974).
- [8] M. G. Castellano, G. Torrioli, C. Cosmelli, A. Costantini, F. Chiarello, P. Carelli, G. Rotoli, M. Cirillo, and R. L. Kautz, Phys. Rev. B **54**, 15417 (1996).
- [9] P. Agren, K. Andersson, and D. B. Haviland, J. Low Temp. Phys. **124**, 291 (2001).
- [10] P. Agren, *Cooper pair transport and Coulomb blockade in one dimensional Josephson junction arrays*, Licentiate thesis, KTH, Stockholm, Sweden. Available at: <http://www.nanophys.kth.se> (2000).
- [11] D. Haviland, K. Andersson, and P. Agren, J. Low Temp. Phys. **118**, 733 (2000).
- [12] R. Fazio and H. Van Der Zant, Physics Reports **355** (2001).
- [13] K. Andersson, *A Cooper pair turnstile made from a one dimensional array of Josephson junctions*, Licentiate thesis, KTH, Stockholm, Sweden. Available at: <http://www.nanophys.kth.se> (1999).
- [14] P. Delsing, C. D. Chen, D. B. Haviland, Y. Harada, and T. Claesson, Phys. Rev. B **50**, 3959 (1994).
- [15] A. B. Zorin, Rev. Sci. Instrum. **66**, 4296 (1995).
- [16] R. L. Kautz, G. Zimmerli, and J. M. Martinis, J. Appl. Phys. **73**, 2386 (1993).
- [17] M. H. Devoret, J. M. Martinis, and J. Clarke, Phys. Rev. Lett. **55**, 1908 (1985).